Atmospheric
Chemistry
and Physics
Discussions

Open Access

Deuterium excess in atmospheric water vapor of a Mediterranean coastal wetland: regional versus local signatures

H. Delattre, C. Vallet-Coulomb, and C. Sonzogni

Aix-Marseille Université, CNRS, IRD, CEREGE UM34, 13545 Aix-en-Provence, France

Correspondence to: C. Vallet-Coulomb (vallet@cerege.fr)

Discussion Paper | Discussion Paper | Discussion Paper | Discussion Paper

ACPD

15, 1703–1746, 2015

Deuterium excess in atmospheric water vapor

H. Delattre et al.

Title Page

Abstract	Introduction
Conclusions	References
Tables	Figures

◀ ▶

◀ ▶

Back | Close

Full Screen / Esc

Printer-friendly Version

Interactive Discussion

Abstract

Stable isotopes of the water vapor represent a powerful tool for tracing atmospheric vapor origin and mixing processes. Laser spectrometry recently allowed high time resolution measurements, but despite an increasing number of experimental studies, there is still a need for a better understanding of the main drivers of isotopic signal variability at different time scales. We present results of in situ measurements of δ^{18}O and δD during 36 consecutive days in summer 2011 in atmospheric vapor of a Mediterranean coastal wetland exposed to high evapotranspiration (Camargue, Rhône River delta, France). A calibration protocol was tested and instrument stability was analysed over the period. The mean composition of atmospheric vapor during the campaign is δ^{18}O = -14.66‰ and δD = -95.4‰, with δ_v data plotting clearly above the local meteoric water line, and an average deuterium excess (d_v) of 21.9‰. At daily time step, we show a clear separation of isotopic characteristics with respect to the air mass back trajectories, with the Northern air masses providing depleted compositions (δ^{18}O = -15.83‰, δD = -103.5‰) compared to Mediterranean air masses (δ^{18}O = -13.13‰, δD = -86.5‰). There is also a clear separation between d_v corresponding to these different air mass origins, but not in the same direction as was previously evidenced from regional rainfall data, with higher d_v found for Northern air masses (23.2‰) than for Mediterranean air masses (18.6‰). Based on twenty-four average hourly data, we propose a depiction of typical daily evolution of water vapor isotopic composition. High diurnal variations in d_v is attributed to a dominant control of evapotranspiration, over entrainment of free atmosphere. Daily cycles in d_v are more pronounced for Mediterranean than for North Atlantic air mass origin and are discussed in terms of local evapotranspiration versus regional signatures. We calculate the composition of the vapor source that produces the day-time increase in d_v for the different air mass origins, and propose an atmospheric water and isotopic mass balance.

Deuterium excess in atmospheric water vapor

H. Delattre et al.

1   Introduction

At the global scale, an acceleration of the hydrological cycle is expected in response to climate change, with an intensification of both precipitation and evaporation. This effect has been recognized for the ocean (Dai et al., 2009), but less conclusive patterns appear for continental surfaces, especially because of the complex behaviour of land evapotranspiration (Brutsaert, 2006; Fu et al., 2009; Jung et al., 2010; Ohmura and Wild, 2002; Roderick and Farquhar, 2002; Roderick et al., 2007). The response of evapotranspiration to climate change is controlled both by climatic and by hydrological parameters. Climate determines the atmospheric evaporative demand (potential evapotranspiration), while hydrology controls surface water availability, thus limiting actual evapotranspiration. In addition, continental vapor is involved in land-atmosphere feedbacks such as atmospheric water recycling: high continental evapotranspiration may contribute to regional rainfall in contexts of tropical rainforest (Brubaker et al., 1993; Eltahir and Bras, 1996; van der Ent et al., 2010) or large scale irrigation (Boucher et al., 2004; Tuinenburg et al., 2012), or may even reduce potential evapotranspiration (Destouni et al., 2010; Tuinenburg et al., 2012). A better understanding of the atmospheric component of the water cycle and of the potential contribution of wetlands evaporation to the regional water budget is thus important to anticipate the impact of global change, in particular in Mediterranean regions where more frequent droughts are expected.

Isotopic composition of atmospheric water vapor (subsequently called δ_v) represents a great opportunity to explore land-atmosphere interactions, as the addition of moisture originating from land evapotranspiration induces a modification of the isotopic content of the background vapor (Gat, 2000; Risi et al., 2013; Worden et al., 2007; Yamanaka and Shimizu, 2007). In addition, isotope tracers are now often incorporated into climate models (Hoffmann et al., 1998; Joussaume et al., 1984; Lee and Fung, 2008; Risi et al., 2010, 2012; Sturm et al., 2005; Tindall et al., 2009; Werner et al., 2011; Yoshimura et al., 2011) in order to improve the representation of land-atmosphere interactions and

feedbacks. A major challenge is thus to propose robust databases, and associated methodology for data acquisition and interpretation.

Laser spectrometers recently opened the door towards the high temporal resolution analysis of δ_v variations, which was not possible with the traditional cold trap method.
5   Whereas cryogenic trapping provides grab samples generally averaging a couple of hours, laser spectrometry performs continuous (every 5 to 7 s) measurements of δ_v. This technology offers new insights into processes that affect the isotopic composition of atmospheric water vapor and the number of studies based on continuous ground level isotope measurements over multi-week periods is continuously increasing, either
10   using Tunable Diode Laser (TDL; Griffis et al., 2011; Lee et al., 2006; Welp et al., 2012; Wen et al., 2010, 2012), Off-Axis Integrated Cavity Output Spectroscopy (OA-ICOS; Farlin et al., 2013; Steen-Larsen et al., 2013; Sturm and Knohl, 2010; Sunmonu et al., 2012) or Wavelength-Scanned Cavity Ring-Down Spectroscopy (WS-CRDS; Galewsky et al., 2011; Noone et al., 2011; Steen-Larsen et al., 2013, 2014; Tremoy et al., 2012).
15   Among these experiments are some low latitude studies which have focused on the tracing of tropical or sub-tropical convective activity in West Africa (Tremoy et al., 2012) or in South America (Galewsky et al., 2011). In mid latitudes (Farlin et al., 2013; Noone et al., 2011), or high latitudes (Steen-Larsen et al., 2013), several studies have explored atmospheric mixing processes at different time scales. Isotopes have also been used
20   for partitioning evapotranspiration into plant transpiration and direct evaporation, as the associated fractionations are different (Griffis et al., 2011; Lai et al., 2006; Sun et al., 2014; Wang et al., 2010; Yakir and Sternberg, 2000), for a better understanding of the role of ecosystems in the hydrological cycle in the context of climate change (Wang et al., 2013).

25   However, the number of studies remains limited because of technical difficulties associated with field-deployed long-term measurements. Except for some work based on cold trap sampling (Angert et al., 2008; Jacob and Sonntag, 1991; Williams et al., 2004), there is to our knowledge a single high time-resolution study published for a European site (Aemisegger et al., 2014) and none at all treating Mediterranean areas.

In addition, there is a need for dual tracer databases, in order to use the deuterium excess signal (Dansgaard, 1964) as an additional indicator of atmospheric processes. Indeed, d_v allows to investigate processes that modify δ_v other than simple Rayleigh rainout processes, such as the climatic conditions of marine sources of vapor (Jouzel et al., 2013), or the secondary addition of continental moisture (Lai and Ehleringer, 2011; Welp et al., 2012).

In this paper, we provide results obtained in a Mediterranean humid zone on 36 consecutive days during summer 2011, using WS-CRDS technology. The study site is exposed to high evaporation, and a large range of surface water composition is submitted to evaporation and evapotranspiration, from the nearby enriched sea surface to the paddy-field areas irrigated with the isotopically depleted Rhône River water. Before analysing our results, we present technical aspects of measurement calibration and validation. We then analyse the day-to-day variations of δ_v and d_v in relation to climatic parameters and the air mass back trajectories. Finally, average hourly variations are explored in order to depict their driving factors and the influence of local surface fluxes.

2 Data acquisition

2.1 Protocols

Continuous in situ measurements of the isotopic composition of atmospheric water vapor ($\delta^{18}O$ and δD) were performed during summer 2011 between 20 July and 24 August, at 1.75 m height and approximately 170 m from the East border of the Vaccarès lagoon (Fig. 1), using Wavelength-Scanned Cavity Ring-Down Spectroscopy (WS-CRDS). The instrument we use is the Picarro L1102-i isotopic liquid water and water vapor analyser (Picarro Inc., Sunnyvale, California, USA), which measures the isotopic composition of atmospheric water vapor every 5 to 7 s. Installed in an air-conditioned room, the analyser is connected to an outside air intake. As water vapor may be sticky on the walls of any tubing, a bypass configuration is used to bring the

air in quickly, at a rate of $6\,\mathrm{L\,min^{-1}}$ (with a Laboport vacuum pump N86 KN.18) through PVC tubing, in order to avoid any fractionation. The analyser then subsamples this air at a rate lower than $0.4\,\mathrm{L\,min^{-1}}$.

Calibration of laser measurements is performed according to laboratory liquid standards, and a three-way valve allows switching between the introduction of ambient air and vapor from the liquid sample vaporizer (vaporization module V1102-i adjusted to $110\,^{\circ}\mathrm{C}$ for flash vaporization to avoid fractionation). We used three laboratory standards whose isotopic spans a range of values including the value expected in the atmosphere of the Camargue (Table 1). $1.8\,\mu\mathrm{L}$ of water standards are introduced is injected into the vaporizer using an autosampler (CTC Analytics LEAP Technologies HTC PAL autosampler) with a SGE $5\,\mu\mathrm{L}$ syringe. We used synthetic air as the dry carrier gas (water content $< 45\,\mathrm{ppmv}$) delivered at a pressure of $2.5 \pm 0.5\,\mathrm{psi}$. The analyser takes about nine minutes to perform approximately 40 measurements per injection, and these results are then averaged by the software. Between each injection, the syringe is cleaned with 1-methyl-2-pyrrolidinone (NMP) solvent wash. Our laboratory successfully participated in the IAEA 2011 proficiency test on routine analysis of $\delta^{18}\mathrm{O}$ and $\delta\mathrm{D}$ in liquid water (Wassenaar et al., 2012).

Previous studies have shown that optical spectrometric methods can induce a dependence of isotopic measurements on water vapor concentration (Gupta et al., 2009; Johnson et al., 2011; Schmidt et al., 2010; Tremoy et al., 2011). This does not affect liquid sample measurements, since the water quantity introduced into the analyser through the vaporizer is very nearly constant, but important variations of vapor content do occur when analysing ambient atmosphere, making it necessary to correct optical measurements. We have evaluated the concentration dependence of our instrument for a large range of water concentrations, and for different isotopic compositions using our three standards (Fig. 2). In addition, for routine analysis, an evaluation of the water concentration effect is performed at approximately $24\,\mathrm{h}$ intervals with the more depleted standard (Standard 1) whose isotopic composition is close to the atmosphere of the Camargue. The autosampler is set to perform six injections of 0.9, 1.6 and $2.0\,\mu\mathrm{L}$ in

the vaporization module to obtain three water vapor concentrations ranging from about 8000 to 28 000 ppmv, comprising values expected in the study area. In addition, calibration for isotopic composition is performed at least every 24 h with our three standards. For each standard, the autosampler is set to perform six injections of 1.8 µL in the vaporization module, corresponding to a water vapor concentration of approximately 20 000 ppmv. The first two injections are disregarded to remove the memory effect, and the last four injections are averaged to obtain the δ^{18}O and δD measurements of each standard.

Gaps in time series correspond to calibration periods, but may also reflect accidental power cuts or data eliminated during episodes of condensation in the tubing. This latter problem was detected thanks to the use of transparent air tubing, and was easily recognizable a posteriori through the abnormally smooth shape of the water vapor concentration curve. A heating cable was then used to avoid any condensation such as may occur when a negative temperature gradient exists between the sampling point and the inlet of the analyser.

2.2 Dependence on water vapor concentration

It has been shown that the dependence of WS-CRDS isotopic measurements on water vapor concentration is instrument-dependent (Tremoy et al., 2011). The concentration dependence of our instrument, evaluated for a large range of concentrations (Fig. 2), showed a linear response in the range of water vapor concentration measured in the atmosphere of the Camargue (from 9000 to 28 000 ppmv), with the relationship deviating slightly from the linear trend at very low and high water vapor concentrations. For δ^{18}O of standards 2 and 3 there is no concentration effect, but a small dependence did appear for the more depleted standard (-0.33‰ 10 000 ppmv^{-1}; $R^2 = 0.75$). For δD, we found significant regression coefficients ($R^2 = 0.98$, 0.99 and 1.00 for standards 1, 2 and 3 respectively), and the slope of the dependence was only slightly different between standards (between 7.8 and 8.1‰ 10 000 ppmv^{-1}).

H. Delattre et al.

Title Page

Abstract | Introduction

Conclusions | References

Tables | Figures

|◄ | ►|

◄ | ►

Back | Close

Full Screen / Esc

Printer-friendly Version

Interactive Discussion

This justifies the use of only one standard (Standard 1) to perform the very time-consuming daily calibration of the water concentration effect (160 min for a 3-point calibration). Measurements are corrected for concentration dependence before applying the isotopic calibration in order to drive back atmospheric measurements to the water vapor concentration $w_{reference}$ at which standards are measured, as follows (Schmidt et al., 2010):

$$\delta_{reference} = \delta_{observed} + m \cdot (w_{reference} - w_{observed}) \tag{1}$$

where $\delta_{reference}$ (‰) is the reference δ value at $w_{reference}$ (20 000 ppmv in our case); $\delta_{observed}$ (‰) is the observed δ value at $w_{observed}$ (ppmv) the observed concentration; m (‰ ppmv^{-1}) is the slope of the concentration dependence (Table 2).

2.3 Instrument stability

To evaluate the long-term stability of our instrument, statistics were calculated on raw delta values measured on our three standards during the entire measurement campaign (Table 1). Results show that the long-term variability is very low, but a regular calibration is nevertheless performed. Variability of both calibrations (for water vapor concentration and isotopic composition) is shown in Table 2. For δ^{18}O, the calibration for concentration appears highly variable but often flat (no concentration effect), resulting in a linearity which is not always significant ($0.26 \leq R^2 \leq 1.00$). Thus, δ^{18}O was corrected only when the concentration dependence was significant. For δD, the regression is slightly variable in the long-term, and its linearity is always significant ($0.89 \leq R^2 \leq 0.99$). For daily calibration in isotopic composition, linear regressions between raw measured values and absolute standard compositions are established as follows for δ^{18}O and δD:

$$\delta_{calibrated} = slope \cdot \delta_{measured} + intercept \tag{2}$$

Regressions are stable in the long-term (Table 2), and their linearity is always significant ($R^2 = 1.00$). Accuracy and precision of our measurements, estimated by considering

standard 2 as a sample which has been calibrated with standards 1 and 3, show good results (Table 3).

3   Climatic data

We collected and analysed three rainfall samples corresponding to four rainfall events (25, 26, 27 July, 7 August 2011). These samples account for a total of 7.6 mm of the 9.6 mm of cumulated rainfall during the measurement campaign; the remaining 2mm correspond to eight very small events between 14 and 23 August (not sampled). Hourly air temperature and relative humidity were measured at the study site. Hourly wind speed and daily potential evapotranspiration (Penman-Monteith PET) were obtained from a meteorological station located 400 m far from the site of isotopic measurements. In addition, surface temperature was also measured in the Vaccarès lagoon at hourly time-step.

Backward three-dimensional trajectories were computed for each individual day with the Internet-based NOAA HYSPLIT Trajectory Model (http://ready.arl.noaa.gov/HYSPLIT.php), using GDAS (Global Data Assimilation System) meteorological data. Trajectories were parameterized to end up at the station location at 12:00 UTC, at three heights of 50, 100 and 500 m above ground level, with a total back run time long enough to get to the oceanic source (maximum of 144 h). Planetary boundary layer heights were obtained from GDAS meteorological data (3 h time step). They were extracted and interpolated to our specific station using the MeteoInfo software (www.meteothinker.com).

4   Results and discussion

The mean composition of atmospheric water vapor during the campaign is $\delta^{18}O = -14.66$‰, $\delta D = -95.4$‰ and $d_v = 21.9$‰, with significant daily variations, from $\delta^{18}O = -19.22$ to -9.96‰ and $\delta D = -125.2$ to -61.7‰, while d_v varies between 7.8 and

31.2 ‰. Substantial day-to-day variations are observed, which appear higher than the hourly variations, except for d_v, which presents hourly variations higher than those observed at daily time step (Fig. 3).

4.1 Time series analysis

4.1.1 Correlations between isotope data and climatic parameters at daily time-step: evidence for different vapor sources

In order to explore the relevant time scales for interpreting isotopic data in terms of synoptic and mesoscale meteorology versus local influences, a first analysis of our data is based on daily averages. Quite good correlations are found between daily values of δ_v and climatic parameters (Table 4), the best fit being with the mixing ratio q, ($R^2 = 0.72$ and 0.62 for $\delta^{18}O$ and δD respectively). Such a correlation could result from the case of simple Rayleigh rainout processes, where condensation phases progressively remove water from the atmosphere and deplete the remaining atmospheric vapor in heavy isotopes, inducing a relation between δ_v and q (Lee et al., 2006; Wen et al., 2010). The progressive depletion in heavy isotopes follows a temperature decrease, and should also result in a correlation between δ_v and T, and subsequently between rainfall isotope content (δ_p) and T, which has led to the establishment of the isotopic thermometer (Dansgaard, 1964; Jouzel et al., 1997). Our data show a relation between δ_v and T (Table 4, Fig. 3) close to the isotopic thermometer: $\Delta\delta^{18}O/\Delta T = 0.53\,‰\,°C^{-1}$ (Jouzel et al., 1997), but the correlation is relatively poor ($R^2 = 0.30$), indicating more complex processes, as was observed during a long-term Swiss survey in which $\delta_v - T$ correlation was degraded during summer because of the admixture of vapor originating from plant transpiration (Jacob and Sonntag, 1991). The good correlation between δ_v and q more probably suggests mixing between air masses characterized by different vapor compositions and concentrations as could result from different marine origins, and/or from the addition of continental vapor into the marine air mass during its travel over land.

H. Delattre et al.

Title Page

Abstract　　Introduction

Conclusions　　References

Tables　　Figures

◄　　►

◄　　►

Back　　Close

Full Screen / Esc

Printer-friendly Version

Interactive Discussion

Deuterium excess is a good indicator of such vapor mixing processes, since it is hardly modified by the Rayleigh process, except for the influence of the non-linearity in the definition of deuterium excess. Indeed, the delta-notation approximation induces a small shift when there is a large decrease in δ^{18}O and δD (Angert et al., 2008; Gat et al., 1996; Welp et al., 2012), and as a consequence d_v is thus not totally conservative during rainout. In the observed range of δ^{18}O (from −11 to −18‰), we have estimated this effect to induce a 2.5‰ increase in d_v, while the substantial variations in d_v observed in our daily data are significantly higher (from 15 to 26‰), allowing the use of d_v as a tracer of different vapor masses.

The significance of deuterium excess in terms of vapor sources comes from the fact that it is determined by the isotopic fractionation that occurs during evaporation, and more precisely by its variable kinetic component, which depends on local climatic conditions (Craig and Gordon, 1965; Gonfiantini, 1986). Deuterium excess is initially determined by the conditions of vapor formation at the oceanic initial source (Armengaud et al., 1998; Jouzel et al., 2013; Merlivat and Jouzel, 1979; Steen-Larsen et al., 2013), d_v being higher for lower humidity conditions over the ocean, or for higher sea surface temperature. It may then be modified during the air mass trajectory over land, by the addition of vapor of continental origin (Angert et al., 2008; Lai and Ehleringer, 2011; Welp et al., 2012). The contribution of this "secondary" vapor produces higher d_v, as was illustrated in a multi-site study by Welp et al. (2012) for two of their six sites located near large bodies of water, through correlations between d_v and relative humidity. Our data also present a good correlation between d_v and RH ($R^2 = 0.51$), with a slope (-0.23‰ %$^{-1}$) in the range of those observed by Welp et al. (2012) (between -0.22 and -0.36‰ %$^{-1}$).

However, relative humidity combines both temperature and water concentration, and q, which purely reflects the amount of water, can better describe an air mass. The correlation between q and d_v ($R^2 = 0.54$) thus indicates the mixing of air masses characterised by different atmospheric vapor sources.

H. Delattre et al.

4.1.2 Influences of backward trajectories

In order to examine the link between the isotopic characteristics of vapor and the air mass trajectories since its oceanic origin, data were classified based on the three main regional features schematically represented in Fig. 1. Corresponding average characteristics were calculated (Table 5). It appears that T, q and V roughly reflect synoptic weather conditions related to origin of air masses, and each synoptic situation presents different isotopic characteristics of vapor. Air masses coming from the North Atlantic are associated with cold, dry and strong winds, and have isotopically depleted vapor and high d_v, while those from the Mediterranean are associated on the contrary with warm, wet and light winds, and have isotopically enriched vapor and low d_v. The Bay of Biscay is an intermediate situation. These observations remain in good agreement with slope signs of the correlations summarised in Table 4.

It appears that the greater the distance over land (Fig. 1), the more depleted is δ_v and the higher is d_v (Table 5). The northern trajectory corresponds to a "Mistral" situation: a typical cold, dry and strong north-northwest wind that affects the north of the occidental Mediterranean basin 130 days a year on average. The air mass is gradually dried out by rainout processes over land and accelerated in the Rhône Valley and acquires a depleted isotopic signature. On the contrary, an air mass travelling over the Mediterranean Sea with the slight thermal wind or sea breeze coming from the South is moistened and acquires and maintains an enriched isotopic signature.

4.1.3 Comparison with rainfall composition

On first sight, the highest d_v values associated with the North Atlantic trajectories appear surprising, since regional studies based on precipitation composition showed higher deuterium excess for rainfall of Mediterranean origin than for Atlantic (Celle-Jeanton et al., 2001; Gat and Carmi, 1970; Jaunat et al., 2013; Ladouche et al., 2009; Lambs et al., 2013). However, those studies showed values near the global average of 10‰ for rainfall of Atlantic origin, which points to the average humidity conditions

over the oceans, while our vapor data show higher deuterium excess in all climatic conditions: $d_v = 18.6$‰ for Mediterranean air masses and $d_v = 23.2$‰ for North Atlantic air masses, which indicates an important influence of kinetic fractionation during evaporation.

5   Above the Mediterranean Sea, high deuterium excess values in rainfall (Gat and Carmi, 1970) and in atmospheric vapor (Gat et al., 2003) were attributed to conditions of strong kinetic fractionation during seawater evaporation. This corresponded to the influence of dry continental air masses, and was observed in locations close to the shorelines, or further offshore for air masses originating from the European continent.

10   Our data were obtained during a period with low precipitation: 9.6 mm rainfall over the 36-day period, during which four rainfall events were collected. Unfortunately, these rainfall events fall during occasional interruptions of vapor measurements, due either to calibration periods or to accidental power outages, thus preventing a precise comparison between laser data and the theoretical vapor compositions in isotopic equilibrium
15   with rainfall. Nevertheless, equilibrium compositions show roughly the same trends as do measured δ_v variations (Fig. 3), with δ^{18}O slightly higher and δD slightly lower than ground-based measurements. Such differences between precipitation and vapor compositions were also observed by Jacob and Sonntag (1991), who interpreted them as being due to either the partial evaporation of raindrops beneath the cloud-base level,
20   or to the admixture of soil evaporation. Our data indicate the combined influence of both processes. The low deuterium excess found for these rainfall compositions (5.6, 4.5 and 7.0‰ respectively) suggests a probable influence of evaporation in the atmosphere. This evaporation induces an increase in the theoretical equilibrium compositions compared to the initial vapor phase, which is thus consistent with the measured δ_v
25   for δ^{18}O. However, δD is clearly more enriched in ground-based laser measurements than in the vapor from which rainfall was formed, which suggests the influence of local vapor at ground level.

Deuterium excess in atmospheric water vapor

H. Delattre et al.

Title Page

Abstract | Introduction

Conclusions | References

Tables | Figures

◄ | ►

◄ | ►

Back | Close

Full Screen / Esc

Printer-friendly Version

Interactive Discussion

4.1.4 δ^{18}O-δD relationships

Hourly data are scattered in the δ^{18}O$-\delta$D plot distinctly above the local meteoric water line (LMWL, Fig. 4). As evidenced previously from daily data, air masses coming from the North Atlantic and associated with cold, dry and strong winds, display isotopically

5   depleted vapor, and air masses coming from the Mediterranean and associated with warm, wet and light winds, display isotopically enriched vapor. For air masses coming from the Bay of Biscay, a situation previously characterized as intermediate, our data encompass the entire isotopic range. However, the main feature is the distinct separation between nocturnal and diurnal data, with the latter plotting higher above

10   the meteoric lines. This feature is observed for each of the three air masses defined in Sect. 4.1.2. For these classes of data, strong linear fits are evidenced with slopes lower than the characteristic slope of eight which is observed at global scale for the meteoric water line (Fig. 4) (the value of eight is attributed to thermodynamic equilibrium, as it represents the average ratio between D and ^{18}O liquid-vapor fractionation

15   factors). Such low slopes have also been observed in atmospheric vapor from Hawaii (7.02; Bailey et al., 2013), Greenland (between 6.47 and 7.44; Steen-Larsen et al., 2013), Western Siberia (between 5.6 and 7.7; Bastrikov et al., 2014), and in North America (7.5; Berkelhammer et al., 2013), pointing to a general trend of low slopes for depleted vapor data. This can be attributed to the previously described shift in d_v

20   during Rayleigh-type rainout in the case of a large decrease in δ^{18}O and δD, due to the non-linearity in the deuterium excess definition.

4.2 Analysis of average daily variations

4.2.1 Average daily cycles relative to air mass origins

In order to observe the diurnal variations suggested by the night-day separation, 24 h

25   average values of isotopic and climatic data are plotted for the three air mass origins (Fig. 5). A well-pronounced cyclicity appears for d_v in each climatic condition. For

Bay of Biscay origins, the average d_v cycle is very similar to the North Atlantic conditions, with larger standard deviations, suggesting a more variable climatic situation. For Mediterranean conditions, the d_v cycle is higher in amplitude than for North Atlantic conditions, and lower in absolute values, especially during the night. The high standard deviations observed during the last hours of the day correspond to calibration periods for which there are fewer data, but may also be due to transition periods between different synoptic situations. The increase in d_v during the morning is mainly associated with a δD increase, while δ^{18}O variations are smooth. Amplitudes of daily isotopic variations are higher for Mediterranean conditions (9.7, 16.2 and 1.3‰ for d_v, δD and δ^{18}O respectively) than for North Atlantic ones (7.0, 13.1 and 1.1‰ for d_v, δD and δ^{18}O respectively).

From a climatic point of view, the diurnal cycle is mainly represented by temperature and subsequently, by relative humidity. The latter is essentially controlled by temperature variations and it is also interesting to observe mixing ratio variations, which simply reflect the absolute amount of water. Under Mediterranean conditions, a distinct increase of q occurs in the morning, indicating a net addition of local vapor in the atmosphere. Under North Atlantic conditions, the q increase is lower, but still detectable, suggesting that the local vapor input remains. The daily cyclicity of the planetary boundary layer height (PBLH) is specifically related to the different atmospheric conditions. The PBLH attains around 1100 m on average during the afternoon under North Atlantic and Bay of Biscay conditions, with a significant standard deviation. Under Mediterranean conditions, the PBLH is less variable and remains at almost 700 m. Nocturnal values are also very low – less than 100 m – in Mediterranean conditions, compared to 400–500 m in the other weather situations. Low PBLH in Mediterranean conditions corresponds to weak turbulence and air stability resulting from light winds. Under North Atlantic conditions, the higher PBL corresponds to strong turbulent fluxes, associated with strong winds.

4.2.2 Daily variations of d_v controlled by surface ET

The planetary boundary layer (PBL) mass budget over land is mainly controlled by the entrainment of free atmosphere, and PBL height has been shown to scale as the entrainment rate (Medeiros et al., 2005). This means that higher boundary layer heights would induce the "dilution" of surface mass fluxes by free atmosphere, when these surface fluxes (e.g. aerosols, atmospheric pollutants) do not directly depend on climatic factors (Quan et al., 2013). On the other hand, the main driver of the daily PBL growth is the buoyancy flux, which is mainly driven by the surface sensible flux and the latent heat flux, the latter being dominant in wetlands. In terms of water vapor mass budget, this suggests that higher PBL should correspond to higher contribution of both local evaporation and free atmosphere, but their respective contributions remain unknown.

The isotopic signature of atmospheric water vapor is a good means to decipher these two potential origins of water. Both processes influence d_v in the same direction, but not δ_v: delta values are expected to decrease with altitude (Bailey et al., 2013; He and Smith, 1999), so that entrainment of free atmosphere would lead to a decrease of δ_v during the development of PBL (Bailey et al., 2013; Tremoy et al., 2012), while evapotranspiration produces a more enriched vapor. Daily cyclicity in d_v is thus a widely observed feature (Lai and Ehleringer, 2011; Welp et al., 2012; Zhang et al., 2011), but can be explained as a consequence of either the addition of vapor from evapotranspiration or of the entrainment of free atmosphere into the boundary layer. Welp et al. (2012), compared six measurement locations and found both processes to be involved. The d_v daily increase was associated with a $\delta^{18}O$ decrease during the early morning due to entrainment of free atmosphere into the boundary layer during convective mixing, while the subsequent slight $\delta^{18}O$ increase came from evapotranspiration. Unlike the cases exposed by Welp et al. (2012), our data show that the d_v cyclicity during the day is associated with a daily δ_v increase. We can thus conclude that the addition of surface vapor is the dominant process governing the d_v cyclicity during the day.

During the night, the PBL subsidence corresponds to the disappearance of both the surface heat fluxes and entrainment. There is thus no further addition of water vapor to the atmosphere. The large-scale motion becomes dominant and, without changing the total PBL mass, redistributes it horizontally (Medeiros et al., 2005). We can thus interpret the nocturnal isotopic values as representing a regional signal, onto which are superimposed day-time fluxes. The tendencies identified in Sect. 4.1 at daily time step which are interpreted in terms of regional signature, that is to say, depleted (enriched) δ_v and higher (smaller) d_v under North Atlantic (Mediterranean) conditions, are recovered in night-time values (Table 5, Fig. 6).

4.2.3 Composition of surface vapor influx

We focus our discussion on the two most contrasted climatic situations, i.e. Mediterranean and North Atlantic air mass origins. The daily increase in q clearly reflects the addition of surface water vapor to the regional night-time background, and the comparison between isotopic signals and mixing ratio provides information about mixing processes between these two pools of water vapor. Quite good correlations are found between average values of δ_v and $1/q$ for the period of q increase, i.e. 05:00–13:00 UTC for North Atlantic situations and 05:00–10:00 for Mediterranean situations (R^2 values are between 0.85 and 0.96, see Fig. 6). These linear relationships indicate a mixing between two sources of water vapor (Keeling, 1958; Noone et al., 2011; Yakir and Sternberg, 2000; Zhang et al., 2010). In terms of fluxes, the water budget of the PBL is expressed as resulting from the sum of q_0 (the vapor flux corresponding to night-time air mass) and q_{ET} (the vapor flux corresponding to the day-time additional humid air):

$$q_m = q_0 + q_{ET} \tag{3}$$

The mixing equation is as follows (Yakir and Sternberg, 2000):

$$\delta_m = (\delta_0 - \delta_{ET}) \cdot \frac{q_0}{q_m} + \delta_{ET} \tag{4}$$

The mixing trend takes the shape $y = ax + b$ in which $\delta_{ET} = \delta_m$ when $q_0 = 0$, i.e. for $q_m = q_{ET}$ the mixing ratio of the humid air end-member. Determination of the isotopic composition of water vapor source thus necessitates prior knowledge of the additional humid air mixing ratio (Noone, 2012; Noone et al., 2011), although there is some con-
5   fusion concerning use of the mixing model to infer the isotopic composition of the additional vapor. In the original Keeling model, initially proposed to describe the addition of CO_2 into the atmosphere, the isotopic composition of the gas influx is determined using the intercept of the linear fit, i.e. $1/q_m \rightarrow 0$. In this case, CO_2 is added to the atmosphere as pure gas, i.e. as a variable component of the gas mixture, and the end-
10   member corresponding to "pure CO_2" is obtained for $q_m \rightarrow \propto$ (q_0 cannot be null in this case). However, water vapor added into the atmosphere cannot be considered as a pure gas. Since evaporation is a diffusion process which occurs when undersaturated humid air is in contact with the liquid phase, vapor is added to the atmosphere as the influx of a humid air mass (i.e. with dry air flux as a "carrier gas"), and further mixed
15   into the PBL through turbulence, buoyancy, etc. (Farlin et al., 2013; Griffis, 2013; Lee et al., 2012; Yamanaka and Shimizu, 2007; Yepez et al., 2003). Unlike CO_2, the addition of water vapor through evaporation is thus a mixing of two gas mixtures, and the composition of the additional vapor cannot be inferred from the intercept of the linear regression.
20   Our linear fits are robust for both isotopic species and under both climatic situations (Fig. 6). Based on the mixing ratio corresponding to saturation at the water surface temperature, we have calculated the compositions of the surface vapor for both climatic situations: $\delta^{18}O = -12.5\,‰$; $\delta D = -48\,‰$ for North Atlantic conditions, $\delta^{18}O = -11.8\,‰$; $\delta D = -58\,‰$ for Mediterranean conditions. Note that this saturation assumption corre-
25   sponds to limit conditions at the water-atmosphere interface, such that our calculated humid end-member corresponds to a maximum value for the composition of the surface flux.

These results show the high deuterium excess values characterizing the surface vapor ($d_v = 52$ for North Atlantic and 37 for Mediterranean conditions). The contribution

Deuterium excess in atmospheric water vapor

H. Delattre et al.

Title Page

Abstract	Introduction
Conclusions	References
Tables	Figures

|◄ | ►|

◄ | ►

Back | Close

Full Screen / Esc

Printer-friendly Version

Interactive Discussion

of ET has thus a huge effect on regional d_v. In that sense, these results agree with both Welp et al. (2012), indicating that d_v is not a conservative tracer of oceanic sources, and with Aemisegger et al. (2014), indicating that d_v is a good proxy of continental recycling.

4.2.4 $\delta^{18}O$ – δD relationships

In the $\delta^{18}O$ – δD plot, the two clusters of average vapor data are distributed along two mixing lines, defined by the linear regressions applied to the q-increase period of the day (Fig. 7). These linear fits also meet the previously calculated composition of the humid end-member (Fig. 7). Along these mixing lines, data fluctuate between a maximum value corresponding to the maximum flux of local vapor during day-time, and a minimum value corresponding to the end of the night.

It is noteworthy that the night-time evolution of δ_v is slightly shifted to the right, compared to these mixing lines. For the 20:00–06:00 periods, δ_v follows a decreasing trend and fall along a regression line parallel to the LMWL (Fig. 7). As discussed above, night-time PBL mass balance implies no addition of surface flux or free atmosphere, but only a horizontal redistribution of air masses, suggesting that the night-time background represents the averaged composition of the atmosphere. The progressive isotopic depletion observed during the night can be interpreted either as being due to a progressive condensation (since both q and T also decrease progressively), or as resulting from the ongoing mixing of atmosphere in the PBL, progressively adding a dryer and more depleted vapor.

The high d_v value during the night (on average $15.1 \pm 0.5\,‰$ under Mediterranean conditions and $20.9 \pm 0.7\,‰$ under North Atlantic conditions) suggests that the night-time composition represents a mixing between local ET and an air mass which is not influenced by continental vapor ("remote" air mass). Mixing between evaporation flux and remote vapor was also observed in a previous study (Vallet-Coulomb et al., 2008), where δ_v above an evaporative lake surface was reconstructed from the reverse application of the Craig and Gordon model. The authors estimated the "remote" vapor

Deuterium excess in atmospheric water vapor

H. Delattre et al.

Title Page

Abstract | Introduction

Conclusions | References

Tables | Figures

|◄ | ►|

◄ | ►

Back | Close

Full Screen / Esc

Printer-friendly Version

Interactive Discussion

composition from the intercept between the mixing line $\delta_v - \delta_E$ and the MWL (where δ_E is the composition of evaporated vapor). Here, the composition of the remote air unde-fined vapor is also supposed to be on the extension of the $\delta_R - \delta_{ET}$ line towards depleted values, where δ_R represents the average regional composition. The night-time back-

5   ground represents the averaged composition of the atmosphere, but its composition is not constant, and the composition of the remote vapor remains.

4.2.5 δ_v–RH relationships

We observed a correlation between d_v and RH relative to air temperature, with slightly different slopes associated with the climatic situations: $-0.19‰\%^{-1}$, $R^2 = 0.82$ for

10   North Atlantic situations and $-0.25‰\%^{-1}$, $R^2 = 0.90$ for Mediterranean situations, consistent with Welp et al. (2012). However, there is no longer any correlation when using RH relative to the surface temperature measured in the main pond close to our experimental site (not shown). Correlations between d_v and RH come from the depen-dence of the kinetic fractionation on relative humidity which prevails during evapora-

15   tion. It can only be interpreted in terms of evaporation conditions when assuming a stationary state evaporation from a homogeneous vapor source such as in the Craig and Gordon model, or when applying the closure assumption posited by Merlivat and Jouzel (1979). These idealised conditions can be realized in an oceanic environment (Steen-Larsen et al., 2014), or when applying a Lagrangian moisture source diagnos-

20   tic to create homogeneous multi-day time series (Aemisegger et al., 2014). However, our data describe typical daily cyclicities, and thus, primarily reflect evapotranspiration processes in a non-stationary state.

4.2.6   PBL water budget

In order to evaluate the contribution of daily ET flux to the nocturnal atmospheric back-

25   ground, we tentatively estimate the isotopic mass balances. The contribution of the daily evaporation flux to the night-time background is estimated from the amplitude of

isotopic variations, following a simple two-component mixing model:

$$\left(\frac{Q_{ET}}{Q_{BG}}\right)_i = \frac{\delta_{v(max)} - \delta_{v(min)}}{\delta_{ET} - \delta_{v(min)}} \tag{5}$$

where δ_{ET} is the composition of local ET flux previously determined, $\delta_{v(min)}$ and $\delta_{v(max)}$ are, respectively, the minimum (night-time) and maximum (day-time) compositions of atmospheric vapor, and where Q_{ET}/Q_{BG} is the relative contribution of daily vapor flux to the background. We found Q_{ET}/Q_{BG} values of 0.21 for North Atlantic conditions, consistently when using $\delta^{18}O$ and δD compositions, and 0.48 and 0.43 for Mediterranean conditions, when using, respectively, $\delta^{18}O$ and δD mass balances.

Alternatively, the corresponding water mass balance can be estimated from the ratio of daily evapotranspiration to the increase of water mass in the PBL, assuming an homogeneous air column and purely vertical water flux inside the PBL (without consideration of advection or entrainment):

$$\left(\frac{Q_{ET}}{Q_{BG}}\right)_w = \frac{PET}{W_d - W_n} \tag{6}$$

where PET is the daily potential evapotranspiration (mm), as a good proxy of actual ET in a wetland, and where W_d and W_n reflect the amount of water (mm) in the PBL air column during day-time and night-time, respectively. Water masses are calculated in $kg\,m^{-2}$ (equivalent to mm) by assuming a roughly constant mixing ratio (q, in $mol\,mol^{-1}$) in the PBL, as follows:

$$W = M_{H_2O} \cdot q \cdot \frac{P_{atm} \cdot H}{R \cdot T_p} \tag{7}$$

where H is the maximum PBL height (m), T_p is the average potential temperature in the PBL, estimated from surface measurements (K), P_{atm} is the atmospheric pressure (Pa), and M_{H_2O} is the molar mass of water ($kg\,mol^{-1}$). Compared to the Mediterranean

situation, North Atlantic conditions correspond to stronger average potential evapotranspiration rates (5.8 mm day^{-1} versus 3.8 mm day^{-1}, see Table 5), and to a lower daily variation in the total amount of water (8.6 mm day^{-1} versus 11.1 mm day^{-1} for $W_d - W_n$), mainly because the PBL remains high during the night. As a consequence, we found Q_{ET}/Q_{BG} values of 0.66 and 0.34 for North Atlantic and Mediterranean conditions, respectively. We are aware that our water balance relies on rough assumptions relative to the average vertical profiles in the PBL. However, the calculation is only slightly sensitive to temperature and pressure variations, and is sufficient to allow comparison of the order of magnitude obtained from isotope and water mass balances, and thus, to evaluate the robustness of the assumptions on which the PBL water balance is based. For Mediterranean situations, the isotope mass balance indicates a higher proportion of local vapor than does the PBL water balance, which suggests a higher concentration of local vapor in the lower part of the PBL. On the contrary, under North Atlantic conditions, the isotopic contribution of the local flux is substantially lower than the water influx calculated from the PBL water balance, which indicates an addition water inflow from advection and/or entrainment. High wind speed under North Atlantic conditions (2.0 m s^{-1} compared to 0.7 m s^{-1} for Mediterranean conditions) suggests that the local atmosphere is affected by the contribution of dry northward air masses, and that the local isotopic signal is thus "diluted", both by horizontal advection and by entrainment of free atmosphere. The contribution of surface evaporation into the PBL is thus modulated by the contribution of advection to the local water balance.

5 Conclusions

Our results show that daily averages of atmospheric vapor compositions are mainly controlled by synoptic and mesoscale weather conditions, related to air mass origin and trajectory. Cold, dry and strong winds coming from the North bring an isotopically depleted vapor with a high d_v. Inversely, warm, wet and light winds coming from the South bring an isotopically enriched vapor with a lower d_v. In all situations, deuterium

excess is higher than the global average of 10, and higher than deuterium excess measured in rainfall, both when considering the small rainfall events during the campaign, or the long-term average composition of regional precipitation.

Average hourly data clearly indicate that this high deuterium excess results from the contribution of local evapotranspiration. Whatever the synoptic situation, the strong diurnal cycles are essentially driven by evapotranspiration, and the amplitude of the variations is modulated by the ET flux intensity and advection. The robust alignment of our average data in a $\delta_v - 1/q$ plot allowed us to calculate the isotopic composition of the humid end-members, and produced very close results for the two main air mass trajectories. In the $\delta^{18}O$-δD plot, average hourly δ_v fluctuates between a maximum value corresponding to the maximum contribution of local vapor during daytime, and a minimum value, corresponding to the night-time background. The night-time background represents the averaged regional composition of the atmosphere, because the PBL mass is horizontally redistributed during the night, and its high deuterium excess indicates that it is still affected by the contribution of local vapor. We thus show that d_v measured in ground level atmospheric vapor carry the isotopic signature of local evapotranspiration and has lost the signature of its initial oceanic vapor source. Our measurements were performed during a summer high pressure period with high daily PET, and further measurements during low pressure situations would be useful in evaluating whether or not the influence of local surface processes remains dominant. This study provides a framework for depicting the typical daily evolution of water vapor isotopic composition during a 24 h cycle. It may thus be useful when analysing non-averaged data corresponding to particular situations, for a better understanding of land-atmosphere water exchanges.

Full Screen / Esc

Printer-friendly Version

Interactive Discussion

Nationale de Camargue warmly for having welcomed our experiments and contributing to the sampling.

References

Aemisegger, F., Pfahl, S., Sodemann, H., Lehner, I., Seneviratne, S. I., and Wernli, H.: Deuterium excess as a proxy for continental moisture recycling and plant transpiration, Atmos. Chem. Phys., 14, 4029–4054, doi:10.5194/acp-14-4029-2014, 2014.

Angert, A., Lee, J.-E. and Yakir, D.: Seasonal variations in the isotopic composition of near-surface water vapour in the eastern Mediterranean, Tellus B, 60, 674–684, doi:10.1111/j.1600-0889.2008.00357.x, 2008.

Armengaud, A., Koster, R. D., Jouzel, J., and Ciais, P.: Deuterium excess in Greenland snow: Analysis with simple and complex models, J. Geophys. Res., 103, 8947–8953, 1998.

Bailey, A., Toohey, D., and Noone, D.: Characterizing moisture exchange between the Hawaiian convective boundary layer and free troposphere using stable isotopes in water, J. Geophys. Res. Atmos., 118, 8208–8221, doi:10.1002/jgrd.50639, 2013.

Bastrikov, V., Steen-Larsen, H. C., Masson-Delmotte, V., Gribanov, K., Cattani, O., Jouzel, J., and Zakharov, V.: Continuous measurements of atmospheric water vapour isotopes in western Siberia (Kourovka), Atmos. Meas. Tech., 7, 1763–1776, doi:10.5194/amt-7-1763-2014, 2014.

Berkelhammer, M., Hu, J., Bailey, A., Noone, D. C., Still, C. J., Barnard, H., Gochis, D., Hsiao, G. S., Rahn, T. and Turnipseed, A.: The nocturnal water cycle in an open-canopy forest, J. Geophys. Res. Atmos., 118, 10225–10242, doi:10.1002/jgrd.50701, 2013.

Boucher, O., Myhre, G., and Myhre, A.: Direct human influence of irrigation on atmospheric water vapour and climate, Clim. Dyn., 22, 597–603, doi:10.1007/s00382-004-0402-4, 2004.

Brubaker, K. L., Entekhabi, D., and Eagleson, P. S.: Estimation of Continental Precipitation Recycling, J. Clim., 6, 1077–1089, 1993.

Brutsaert, W.: Indications of increasing land surface evaporation during the second half of the 20th century, Geophys. Res. Lett., 33, L20403, doi:10.1029/2006GL027532, 2006.

Celle, H., Daniel, M., Mudry, J., and Blavoux, B: Signal pluie et traçage par les isotopes stables en Méditerranée occidentale. Exemple de la région avignonnaise (Sud-Est de la France), C. R. Acad. Sci. Paris, Earth Planet. Sci., 331, 647–650, 2000.

Celle-Jeanton, H., Travi, Y., and Blavoux, B.: Isotopic typology of the precipitation in the Western Mediterranean region at three different time scales, Geophys. Res. Lett., 28, 1215–1218, 2001.

Craig, H. and Gordon, L. I.: Deuterium and oxygen 18 variations in the ocean and the marine atmosphere, in: Stable Isotopes in Oceanographic Studies and Paleotemperatures, edited by: Tongiorgi, E., 9–130, Spoleto, Italy, 1965.

Dai, A., Qian, T., Trenberth, K. E., and Milliman, J. D.: Changes in Continental Freshwater Discharge from 1948 to 2004, J. Clim., 22, 2773–2792, doi:10.1175/2008JCLI2592.1, 2009.

Dansgaard, W.: Stable isotopes in precipitation, Tellus, 16, 436–468, 1964.

Destouni, G., Asokan, S. M., and Jarsjö, J.: Inland hydro-climatic interaction: Effects of human water use on regional climate, Geophys. Res. Lett., 37, L184402, doi:10.1029/2010GL044153, 2010.

Eltahir, E. A. B. and Bras, R. L.: Precipitation Recycling, Rev. Geophys., 34, 367–378, 1996.

Farlin, J., Lai, C.-T., and Yoshimura, K.: Influence of synoptic weather events on the isotopic composition of atmospheric moisture in a coastal city of the western United States, Water Resour. Res., 49, 3685–3696, doi:10.1002/wrcr.20305, 2013.

Fu, G., Charles, S. P., and Yu, J.: A critical overview of pan evaporation trends over the last 50 years, Clim. Change, 97, 193–214, doi:10.1007/s10584-009-9579-1, 2009.

Galewsky, J., Rella, C., Sharp, Z., Samuels, K., and Ward, D.: Surface measurements of upper tropospheric water vapor isotopic composition on the Chajnantor Plateau, Chile, Geophys. Res. Lett., 38, L17803, doi:10.1029/2011GL048557, 2011.

Gat, J. R.: Atmospheric water balance – the isotopic perspective, Hydrol. Process., 14, 1357–1369, 2000.

Gat, J. R. and Carmi, I.: Evolution of the Isotopic Composition of Atmospheric Waters in the Mediterranean Sea Area, J. Geophys. Res., 75, 3039–3048, 1970.

Gat, J. R., Shemesh, A., Tziperman, E., Hecht, A., Georgopoulos, D., and Basturk, O.: The stable isotope composition of waters of the eastern Mediterranean Sea, J. Geophys. Res., 101, 6441–6451, 1996.

Gat, J. R., Klein, B., Kushnir, Y., Roether, W., Wernli, H., Yam, R., and Shemesh, A.: Isotope composition of air moisture over the Mediterranean Sea: an index of the air–sea interaction pattern, Tellus B, 55, 953–965, 2003.

Gonfiantini, R.: Environmental isotopes in lake studies, in: Handbook of Environmental Isotope geochemistry, edited by: Fritz, P. and Fontes, J. C., 2, Elsevier, Amsterdam, 113–163, 1986.

Griffis, T. J.: Tracing the flow of carbon dioxide and water vapor between the biosphere and atmosphere: A review of optical isotope techniques and their application, Agr. Forest Meteorol., 174–175, 85–109, doi:10.1016/j.agrformet.2013.02.009, 2013.

Griffis, T. J., Lee, X., Baker, J. M., Billmark, K., Schultz, N., Erickson, M., Zhang, X., Fassbinder, J., Xiao, W., and Hu, N.: Oxygen isotope composition of evapotranspiration and its relation to C4 photosynthetic discrimination, J. Geophys. Res., 116, G01035, doi:10.1029/2010JG001514, 2011.

Gupta, P., Noone, D., Galewsky, J., Sweeney, C., and Vaughn, B. H.: Demonstration of high-precision continuous measurements of water vapor isotopologues in laboratory and remote field deployments using wavelength-scanned cavity ring-down spectroscopy (WS-CRDS) technology, Rapid Commun. Mass Spectrom., 23, 2534–2542, doi:10.1002/rcm.4100, 2009.

He, H. and Smith, R. B.: Stable isotope composition of water vapor in the atmospheric boundary layer above the forests of New England, J. Geophys. Res., 104, 11657–11673, 1999.

Hoffmann, G., Werner, M., and Heimann, M.: Water isotope module of the ECHAM atmospheric general circulation model: A study on timescales from days to several years, J. Geophys. Res., 103, 16871–16896, 1998.

Jacob, H. and Sonntag, C.: An 8-year record of the seasonal variation of 2H and 18O in atmospheric water vapour and precipitation at Heidelberg, Germany, Tellus B, 43, 291–300, 1991.

Jaunat, J., Celle-Jeanton, H., Huneau, F., Dupuy, A., and Le Coustumer, P.: Characterisation of the input signal to aquifers in the French Basque Country: Emphasis on parameters influencing the chemical and isotopic composition of recharge waters, J. Hydrol., 496, 57–70, doi:10.1016/j.jhydrol.2013.05.026, 2013.

Johnson, L. R., Sharp, Z. D., Galewsky, J., Strong, M., Van Pelt, A. D., Dong, F., and Noone, D.: Hydrogen isotope correction for laser instrument measurement bias at low water vapor concentration using conventional isotope analyses: application to measurements from Mauna Loa Observatory, Hawaii, Rapid Commun. mass Spectrom., 25, 608–616, doi:10.1002/rcm.4894, 2011.

Joussaume, S., Sadourny, R., and Jouzel, J.: A general circulation model of water isotope cycles in the atmosphere, Nature, 311, 24–29, 1984.

Jouzel, J., Alley, R. B., Cuffey, K. M., Dansgaard, W., Grootes, P., Hoffmann, G., Johnsen, S. J., Koster, R. D., Peel, D., Shuman, C. A., Stievenard, M., Stuiver, M., and White, J.: Validity

Title Page

Abstract | Introduction

Conclusions | References

Tables | Figures

|◄ | ►|

◄ | ►

Back | Close

Full Screen / Esc

Printer-friendly Version

Interactive Discussion

of the temperature reconstruction from water isotopes in ice cores, J. Geophys. Res., 102, 26471–26487, 1997.

Jouzel, J., Delaygue, G., Landais, A., Masson-Delmotte, V., Risi, C., and Vimeux, F.: Water isotopes as tools to document oceanic sources of precipitation, Water Resour. Res., 49, 7469–7486, doi:10.1002/2013WR013508, 2013.

Jung, M., Reichstein, M., Ciais, P., Seneviratne, S. I., Sheffield, J., Goulden, M. L., Bonan, G., Cescatti, A., Chen, J., de Jeu, R., Dolman, A. J., Eugster, W., Gerten, D., Gianelle, D., Gobron, N., Heinke, J., Kimball, J., Law, B. E., Montagnani, L., Mu, Q., Mueller, B., Oleson, K., Papale, D., Richardson, A. D., Roupsard, O., Running, S., Tomelleri, E., Viovy, N., Weber, U., Williams, C., Wood, E., Zaehle, S., and Zhang, K.: Recent decline in the global land evapotranspiration trend due to limited moisture supply, Nature, 467, 951–954, doi:10.1038/nature09396, 2010.

Keeling, C. D.: The concentration and isotopic abundances of atmospheric carbon dioxide in rural areas, Geochim. Cosmochim. Acta, 13, 322–334, 1958.

Ladouche, B., Aquilina, L., and Dörfliger, N.: Chemical and isotopic investigation of rainwater in Southern France (1996–2002): Potential use as input signal for karst functioning investigation, J. Hydrol., 367, 150–164, doi:10.1016/j.jhydrol.2009.01.012, 2009.

Lai, C.-T. and Ehleringer, J. R.: Deuterium excess reveals diurnal sources of water vapor in forest air, Oecologia, 165, 213–223, doi:10.1007/s00442-010-1721-2, 2011.

Lai, C.-T., Ehleringer, J. R., Bond, B. J., and Paw U, K. T.: Contributions of evaporation, isotopic non-steady state transpiration and atmospheric mixing on the $\delta 18O$ of water vapour in Pacific Northwest coniferous forests, Plant, Cell Environ., 29, 77–94, 2006.

Lambs, L., Moussa, I., and Brunet, F.: Air Masses Origin and Isotopic Tracers: A Study Case of the Oceanic and Mediterranean Rainfall Southwest of France, Water, 5, 617–628, doi:10.3390/w5020617, 2013.

Lee, J.-E. and Fung, I.: "Amount effect" of water isotopes and quantitative analysis of post-condensation processes, Hydrol. Process., 22, 1–8, doi:10.1002/hyp.6637, 2008.

Lee, X., Smith, R., and Williams, J.: Water vapour 18O/16O isotope ratio in surface air in New England, USA, Tellus B, 58, 293–304, doi:10.1111/j.1600-0889.2006.00191.x, 2006.

Lee, X., Huang, J., and Patton, E. G.: A Large-Eddy Simulation Study of Water Vapour and Carbon Dioxide Isotopes in the Atmospheric Boundary Layer, Bound.-Lay. Meteorol., 145, 229–248, doi:10.1007/s10546-011-9631-3, 2012.

Deuterium excess in atmospheric water vapor

H. Delattre et al.

Title Page

Abstract	Introduction
Conclusions	References
Tables	Figures

◀◀   ▶▶

◀   ▶

Back   Close

Full Screen / Esc

Printer-friendly Version

Interactive Discussion

Medeiros, B., Hall, A., and Stevens, B.: What Controls the Mean Depth of the PBL?, J. Clim., 18, 3157–3172, 2005.

Merlivat, L. and Jouzel, J.: Global Climatic Interpretation of the Deuterium-Oxygen 18 Relationship for Precipitation, J. Geophys. Res., 84, 5029–5033, 1979.

Noone, D.: Pairing Measurements of the Water Vapor Isotope Ratio with Humidity to Deduce Atmospheric Moistening and Dehydration in the Tropical Midtroposphere, J. Clim., 25, 4476–4494, doi:10.1175/JCLI-D-11-00582.1, 2012.

Noone, D., Galewsky, J., Sharp, Z. D., Worden, J., Barnes, J., Baer, D., Bailey, A., Brown, D. P., Christensen, L., Crosson, E., Dong, F., Hurley, J. V., Johnson, L. R., Strong, M., Toohey, D., Van Pelt, A., and Wright, J. S.: Properties of air mass mixing and humidity in the subtropics from measurements of the D/H isotope ratio of water vapor at the Mauna Loa Observatory, J. Geophys. Res., 116, D22113, doi:10.1029/2011JD015773, 2011.

Ohmura, A. and Wild, M.: Is the Hydrological Cycle Accelerating?, Science, 298, 1345–1346, doi:10.1126/science.1078972, 2002.

Quan, J., Gao, Y., Zhang, Q., Tie, X., Cao, J., Han, S., Meng, J., Chen, P., and Zhao, D.: Evolution of planetary boundary layer under different weather conditions , and its impact on aerosol concentrations, Particuology, 11, 34–40, doi:10.1016/j.partic.2012.04.005, 2013.

Risi, C., Bony, S., Vimeux, F., and Jouzel, J.: Water-stable isotopes in the LMDZ4 general circulation model: Model evaluation for present-day and past climates and applications to climatic interpretations of tropical isotopic records, J. Geophys. Res., 115, D12118, doi:10.1029/2009JD013255, 2010.

Risi, C., Noone, D., Worden, J., Frankenberg, C., Stiller, G., Kiefer, M., Funke, B., Walker, K., Bernath, P., Schneider, M., Wunch, D., Sherlock, V., Deutscher, N., Griffith, D., Wennberg, P. O., Strong, K., Smale, D., Mahieu, E., Barthlott, S., Hase, F., García, O., Notholt, J., Warneke, T., Toon, G., Sayres, D., Bony, S., Lee, J., Brown, D., Uemura, R. and Sturm, C.: Process-evaluation of tropospheric humidity simulated by general circulation models using water vapor isotopologues: 1. Comparison between models and observations, J. Geophys. Res., 117, D05303, doi:10.1029/2011JD016621, 2012.

Risi, C., Noone, D., Frankenberg, C., and Worden, J.: Role of continental recycling in intraseasonal variations of continental moisture as deduced from model simulations and water vapor isotopic measurements, Water Resour. Res., 49, 4136–4156, doi:10.1002/wrcr.20312, 2013.

Roderick, M. L. and Farquhar, G. D.: The Cause of Decreased Pan Evaporation over the Past 50 Years, Science, 298, 1410–1411, doi:10.1126/science.1075390, 2002.

Title Page

Abstract | Introduction

Conclusions | References

Tables | Figures

|◄ | ►|

◄ | ►

Back | Close

Full Screen / Esc

Printer-friendly Version

Interactive Discussion

Roderick, M. L., Rotstayn, L. D., Farquhar, G. D., and Hobbins, M. T.: On the attribution of changing pan evaporation, Geophys. Res. Lett., 34, L17403, doi:10.1029/2007GL031166, 2007.

Schmidt, M., Maseyk, K., Lett, C., Biron, P., Richard, P., Bariac, T., and Seibt, U.: Concentration effects on laser-based δ18O and δ2H measurements and implications for the calibration of vapour measurements with liquid standards, Rapid Commun. Mass Spectrom., 24, 3553–3561, doi:10.1002/rcm.4813, 2010.

Steen-Larsen, H. C., Johnsen, S. J., Masson-Delmotte, V., Stenni, B., Risi, C., Sodemann, H., Balslev-Clausen, D., Blunier, T., Dahl-Jensen, D., Ellehøj, M. D., Falourd, S., Grindsted, A., Gkinis, V., Jouzel, J., Popp, T., Sheldon, S., Simonsen, S. B., Sjolte, J., Steffensen, J. P., Sperlich, P., Sveinbjörnsdóttir, A. E., Vinther, B. M., and White, J. W. C.: Continuous monitoring of summer surface water vapor isotopic composition above the Greenland Ice Sheet, Atmos. Chem. Phys., 13, 4815–4828, doi:10.5194/acp-13-4815-2013, 2013.

Steen-Larsen, H. C., Sveinbjörnsdóttir, A. E., Peters, A. J., Masson-Delmotte, V., Guishard, M. P., Hsiao, G., Jouzel, J., Noone, D., Warren, J. K., and White, J. W. C.: Climatic controls on water vapor deuterium excess in the marine boundary layer of the North Atlantic based on 500 days of in situ, continuous measurements, Atmos. Chem. Phys., 14, 7741–7756, doi:10.5194/acp-14-7741-2014, 2014.

Sturm, K., Hoffmann, G., Langmann, B., and Stichler, W.: Simulation of δ18O in precipitation by the regional circulation model REMOiso, Hydrol. Process., 19, 3425–3444, doi:10.1002/hyp.5979, 2005.

Sturm, P. and Knohl, A.: Water vapor δ^2H and δ^{18}O measurements using off-axis integrated cavity output spectroscopy, Atmos. Meas. Tech., 3, 67–77, doi:10.5194/amt-3-67-2010, 2010.

Sun, S., Meng, P., Zhang, J., Wan, X., Zheng, N., and He, C.: Partitioning oak woodland evapotranspiration in the rocky mountainous area of North China was disturbed by foreign vapor, as estimated based on non-steady-state 18O isotopic composition, Agr. Forest Meteorol., 184, 36–47, doi:10.1016/j.agrformet.2013.08.006, 2014.

Sunmonu, N., Muramoto, K., Kurita, N., Yoshimura, K., and Fujiyoshi, Y.: Characteristics of Seasonal Variation of Near-Surface Water Vapor D/H Isotope Ratio Revealed by Continuous in situ Measurement in Sapporo, Japan, SOLA, 8, 5–8, doi:10.2151/sola.2012-002, 2012.

Deuterium excess in atmospheric water vapor

H. Delattre et al.

Title Page

Abstract | Introduction

Conclusions | References

Tables | Figures

|◀ | ▶|

◀ | ▶

Back | Close

Full Screen / Esc

Printer-friendly Version

Interactive Discussion

Tindall, J. C., Valdes, P. J., and Sime, L. C.: Stable water isotopes in HadCM3: Isotopic signature of El Niño–Southern Oscillation and the tropical amount effect, J. Geophys. Res., 114, D04111, doi:10.1029/2008JD010825, 2009.

Tremoy, G., Vimeux, F., Cattani, O., Mayaki, S., Souley, I., and Favreau, G.: Measurements of water vapor isotope ratios with wavelength-scanned cavity ring-down spectroscopy technology: new insights and important caveats for deuterium excess measurements in tropical areas in comparison with isotope-ratio mass spectrometry, Rapid Commun. mass Spectrom., 25, 3469–3480, doi:10.1002/rcm.5252, 2011.

Tremoy, G., Vimeux, F., Mayaki, S., Souley, I., Cattani, O., Risi, C., Favreau, G., and Oi, M.: A 1-year long δ18O record of water vapor in Niamey (Niger) reveals insightful atmospheric processes at different timescales, Geophys. Res. Lett., 39, L08805, doi:10.1029/2012GL051298, 2012.

Tuinenburg, O. A., Hutjes, R. W. A., and Kabat, P.: The fate of evaporated water from the Ganges basin, J. Geophys. Res., 117, D01107, doi:10.1029/2011JD016221, 2012.

Vallet-Coulomb, C., Gasse, F., and Sonzogni, C.: Seasonal evolution of the isotopic composition of atmospheric water vapour above a tropical lake: Deuterium excess and implication for water recycling, Geochim. Cosmochim. Acta, 72, 4661–4674, doi:10.1016/j.gca.2008.06.025, 2008.

Van der Ent, R. J., Savenije, H. H. G., Schaefli, B., and Steele-Dunne, S. C.: Origin and fate of atmospheric moisture over continents, Water Resour. Res., 46, W09525, doi:10.1029/2010WR009127, 2010.

Wang, L., Caylor, K. K., Villegas, J. C., Barron-Gafford, G. A., Breshears, D. D., and Huxman, T. E.: Partitioning evapotranspiration across gradients of woody plant cover: Assessment of a stable isotope technique, Geophys. Res. Lett., 37, L09401, doi:10.1029/2010GL043228, 2010.

Wang, L., Niu, S., Good, S. P., Soderberg, K., McCabe, M. F., Sherry, R. A., Luo, Y., Zhou, X., Xia, J., and Caylor, K. K.: The effect of warming on grassland evapotranspiration partitioning using laser-based isotope monitoring techniques, Geochim. Cosmochim. Acta, 111, 28–38, doi:10.1016/j.gca.2012.12.047, 2013.

Wassenaar, L. I., Ahmad, M., Aggarwal, P., van Duren, M., Pöltenstein, L., Araguas, L., and Kurttas, T.: Worldwide proficiency test for routine analysis of δ2H and δ18O in water by isotope-ratio mass spectrometry and laser absorption spectroscopy, Rapid Commun. Mass Spectrom., 26, 1641–1648, doi:10.1002/rcm.6270, 2012.

Deuterium excess in atmospheric water vapor

H. Delattre et al.

Title Page

Abstract	Introduction
Conclusions	References
Tables	Figures

|◄ | ►|

◄ | ►

Back | Close

Full Screen / Esc

Printer-friendly Version

Interactive Discussion

Welp, L. R., Lee, X., Griffis, T. J., Wen, X.-F., Xiao, W., Li, S., Sun, X., Hu, Z., Val Martin, M., and Huang, J.: A meta-analysis of water vapor deuterium-excess in the midlatitude atmospheric surface layer, Global Biogeochem. Cy., 26, GB3021, doi:10.1029/2011GB004246, 2012.

Wen, X.-F., Zhang, S.-C., Sun, X.-M., Yu, G.-R., and Lee, X.: Water vapor and precipitation isotope ratios in Beijing, China, J. Geophys. Res., 115, D01103, doi:10.1029/2009JD012408, 2010.

Wen, X.-F., Lee, X., Sun, X.-M., Wang, J.-L., Hu, Z.-M., Li, S.-G., and Yu, G.-R.: Dew water isotopic ratios and their relationships to ecosystem water pools and fluxes in a cropland and a grassland in China, Oecologia, 168, 549–561, doi:10.1007/s00442-011-2091-0, 2012.

Werner, M., Langebroek, P. M., Carlsen, T., Herold, M., and Lohmann, G.: Stable water isotopes in the ECHAM5 general circulation model: Toward high-resolution isotope modeling on a global scale, J. Geophys. Res., 116, D15109, doi:10.1029/2011JD015681, 2011.

Williams, D. G., Cable, W., Hultine, K., Hoedjes, J. C. B., Yepez, E. A., Simonneaux, V., Er-Raki, S., Boulet, G., de Bruin, H. A. R., Chehbouni, A., Hartogensis, O. K., and Timouk, F.: Evapotranspiration components determined by stable isotope, sap flow and eddy covariance techniques, Agr. Forest Meteorol., 125, 241–258, doi:10.1016/j.agrformet.2004.04.008, 2004.

Worden, J., Noone, D., and Bowman, K.: Importance of rain evaporation and continental convection in the tropical water cycle, Nature, 445, 528–532, doi:10.1038/nature05508, 2007.

Yakir, D. and Sternberg, L. da S. L.: The use of stable isotopes to study ecosystem gas exchange, Oecologia, 123, 297–311, 2000.

Yamanaka, T. and Shimizu, R.: Spatial distribution of deuterium in atmospheric water vapor: Diagnosing sources and the mixing of atmospheric moisture, Geochim. Cosmochim. Acta, 71, 3162–3169, doi:10.1016/j.gca.2007.04.014, 2007.

Yepez, E. A., Williams, D. G., Scott, R. L., and Lin, G.: Partitioning overstory and understory evapotranspiration in a semiarid savanna woodland from the isotopic composition of water vapor, Agr. Forest Meteorol., 119, 53–68, doi:10.1016/S0168-1923(03)00116-3, 2003.

Yoshimura, K., Frankenberg, C., Lee, J., Kanamitsu, M., Worden, J., and Röckmann, T.: Comparison of an isotopic atmospheric general circulation model with new quasi-global satellite measurements of water vapor isotopologues, J. Geophys. Res., 116, D19118, doi:10.1029/2011JD016035, 2011.

Deuterium excess in atmospheric water vapor

H. Delattre et al.

Title Page

Abstract	Introduction
Conclusions	References
Tables	Figures

|◀ ▶|

◀ ▶

Back Close

Full Screen / Esc

Printer-friendly Version

Interactive Discussion

Zhang, S., Wen, X., Wang, J., Yu, G., and Sun, X.: The use of stable isotopes to partition evapotranspiration fluxes into evaporation and transpiration, Acta Ecol. Sin., 30, 201–209, doi:10.1016/j.chnaes.2010.06.003, 2010.

Zhang, S., Sun, X., Wang, J., Yu, G., and Wen, X.: Short-term variations of vapor isotope ratios reveal the influence of atmospheric processes, J. Geogr. Sci., 21, 401–416, doi:10.1007/s11442-011-0853-6, 2011.

Deuterium excess in atmospheric water vapor

H. Delattre et al.

Title Page

Abstract | Introduction

Conclusions | References

Tables | Figures

|◄ | ►|

◄ | ►

Back | Close

Full Screen / Esc

Printer-friendly Version

Interactive Discussion

Table 1. Isotopic composition of CEREGE laboratory liquid water standards calibrated with IAEA international standards by laser spectrometry. Corresponding average values and standard deviations of the 40 measurements performed from 20 July to 24 August 2011.

		Calibrated isotopic composition (‰ vs. VSMOW)	Average value of raw measurements (‰)	Standard deviation (‰)
Standard 1	$\delta^{18}O$	−17.12	−13.89	±0.19
	δD	−133.3	−152.6	±2.0
Standard 2	$\delta^{18}O$	−7.85	−4.85	±0.11
	δD	−53.5	−71.1	±1.5
Standard 3	$\delta^{18}O$	0.68	3.41	±0.08
	δD	3.7	−12.8	±1.8

Table 2. Evaluation of the stability of the calibrations in water vapor concentration and isotopic composition, with mean slope and mean intercept ±1 standard deviation obtained for δ^{18}O and δD with n calibrations performed from 20 July to 24 August 2011.

	δ^{18}O	δD
	Water vapor concentration	
Slope	$-0.16 \times 10^{-4} \pm 0.13 \times 10^{-4}$	$6.08 \times 10^{-4} \pm 0.99 \times 10^{-4}$
Intercept	-13.68 ± 0.25	-165.4 ± 2.0
R^2 ($n = 23$)	$0.26 \leq R^2 \leq 1.00$	$0.89 \leq R^2 \leq 0.99$
	Isotopic composition	
Slope	1.03 ± 0.01	0.98 ± 0.01
Intercept	-2.83 ± 0.07	16.3 ± 1.7
R^2 ($n = 40$)	1.00	1.00

Table 3. Accuracy and precision of isotopic liquid water measurement, estimated by considering Standard 2 as a sample which is calibrated with Standards 1 and 3, on a set of 42 calibrations. Accuracy is the deviation of the mean of Standard 2 isotopic composition from its known value, and precision corresponds to the standard deviation.

	$\delta^{18}O$	δD	d
Accuracy (‰)	0.03	0.1	−0.1
Precision (‰)	±0.12	±0.9	±1.3

Table 4. Determination coefficients (R^2) and slopes (S) of linear correlations between daily means of water vapor composition ($\delta^{18}O$, δD, d_v) and air temperature (T), mixing ratio (q), relative humidity (RH).

	$\delta^{18}O$ (‰)		δD (‰)		d_v (‰)	
	R^2	S	R^2	S	R^2	S
T (°C)	0.30	+0.54	0.27	+3.48	0.20	−0.88
q (mmol mol^{-1})	0.72	+0.38	0.62	+2.39	0.54	−0.66
RH (%)	0.64	+0.13	0.55	+0.80	0.51	−0.23

Table 5. Number of days (n) and mean values of $\delta^{18}O$, δD, deuterium excess (d_v), temperature (T), mixing ratio (q), relative humidity (RH), wind speed (V) and potential evapotranspiration (PET) associated with the origin of air masses (Fig. 1).

	North Atlantic (310–360˚)	Mediterranean (110–220˚)	Bay of Biscay (220–310˚)
n	10	13	13
$\delta^{18}O$ (‰)	−15.83	−13.13	−14.90
δD (‰)	−103.5	−86.5	−96.3
d_v (‰)	23.2	18.6	22.9
T (˚C)	21.6	23.3	22.3
q (mmol mol^{-1})	15.0	21.8	18.0
RH (%)	59.5	78.5	68.1
V (m s^{-1})	2.0	0.7	1.6
PET (mm day^{-1})	5.8	3.8	4.9
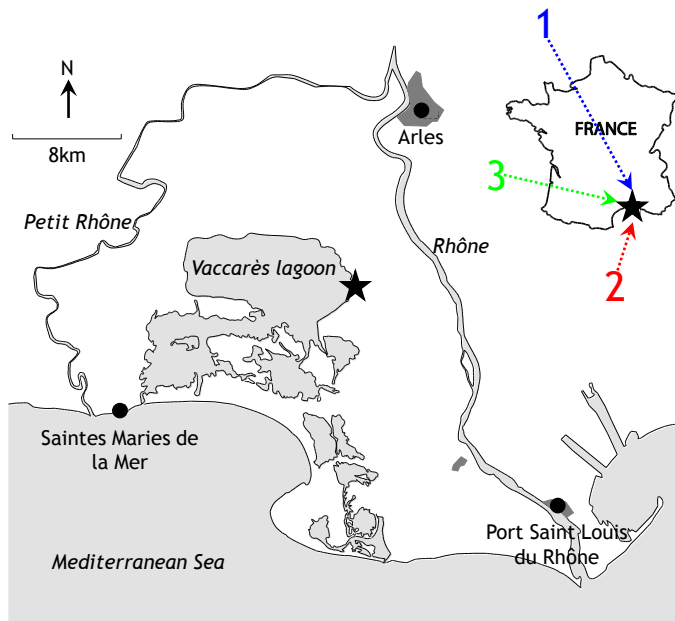
Figure 1. Location of the experimental site (star) in Camargue (Rhône River Delta), 170 m from the Vaccarès lagoon and 12 km from the Mediterranean Sea. Coloured arrows represent the three main origins and trajectories of air masses affecting the study site, (1) North Atlantic, (2) Mediterranean and (3) Bay of Biscay.
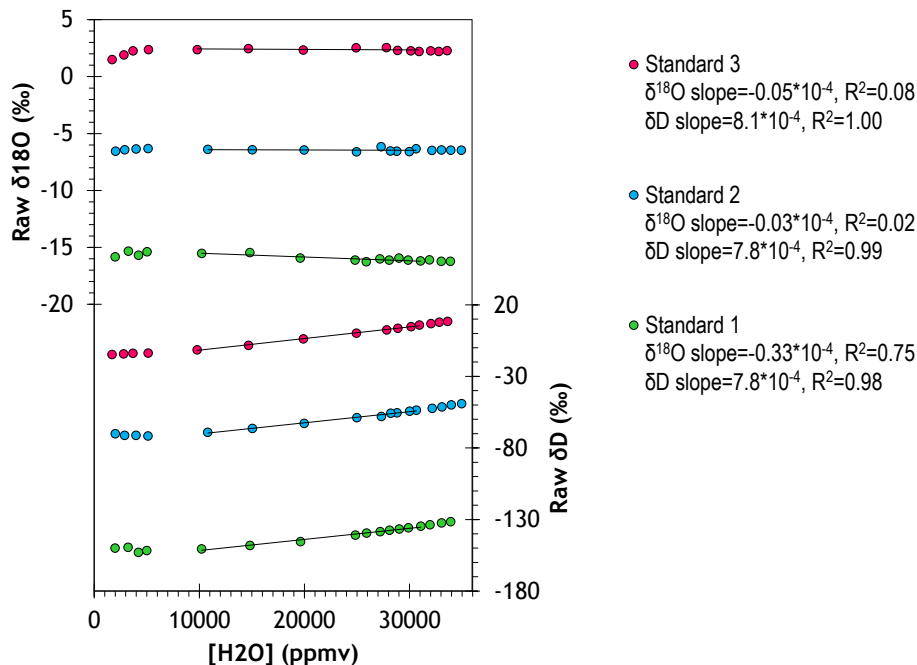
Figure 2. Raw $\delta^{18}O$ and δD of our three laboratory liquid standards measured at various water vapor concentrations. Error bars are smaller than the symbols. Linear regressions within the concentration range encountered in Camargue during the field experiment and associated slopes and determination coefficients are shown.
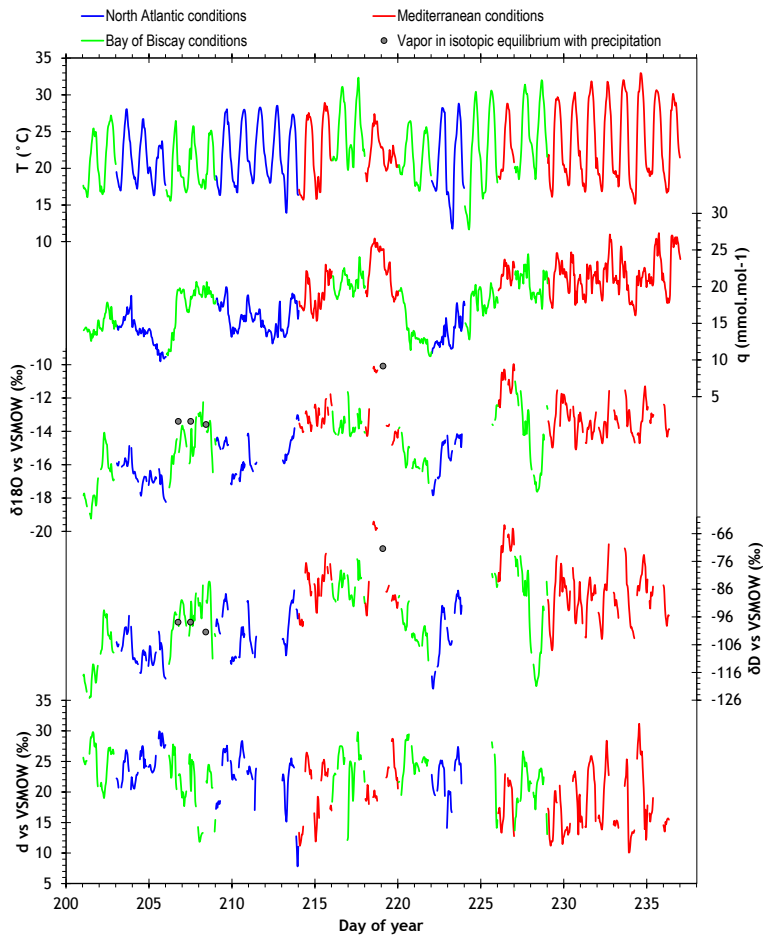
Figure 3. Hourly mean values of air temperature (T), mixing ratio (q), δ^{18}O, δD, deuterium excess (d_v) from 20 July to 24 August 2011 at the experimental site according to air mass origin (see Fig. 1). Grey dots are δ_v calculated in isotopic equilibrium with precipitation.
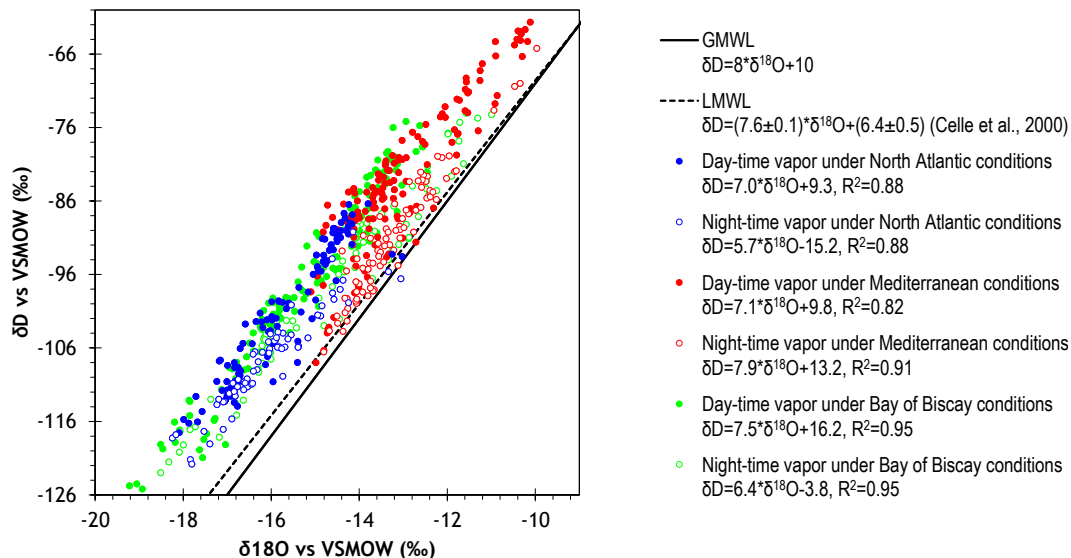
Figure 4. Hourly day-time and night-time isotopic composition of atmospheric water vapor in according to air mass origin. For reference, the GMWL and LMWL are also plotted.
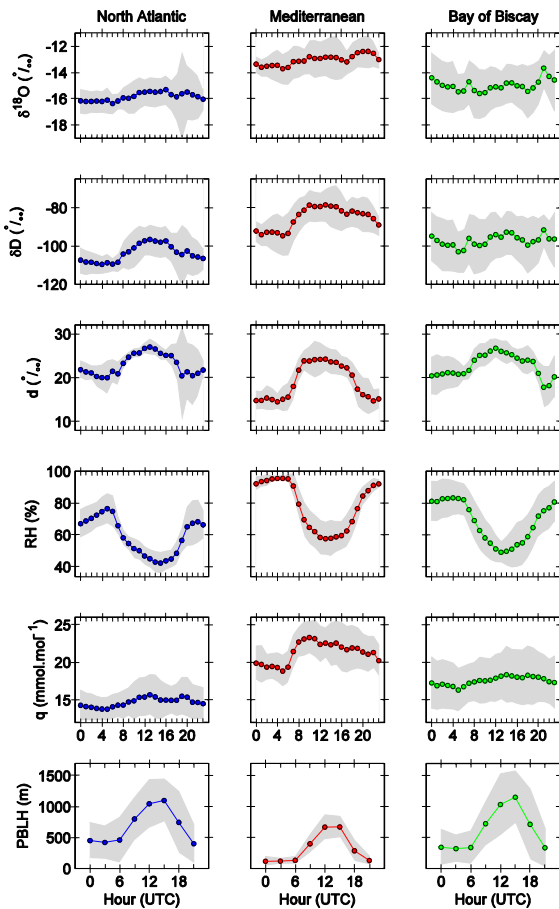
Figure 5. 24 h average values of $\delta^{18}O$, δD, deuterium excess (d), relative humidity (RH), mixing ratio (q) and planetary boundary layer height (PBLH) calculated from 20 July to 24 August 2011 according to air mass origin. Grey shading indicates standard deviation of each average.
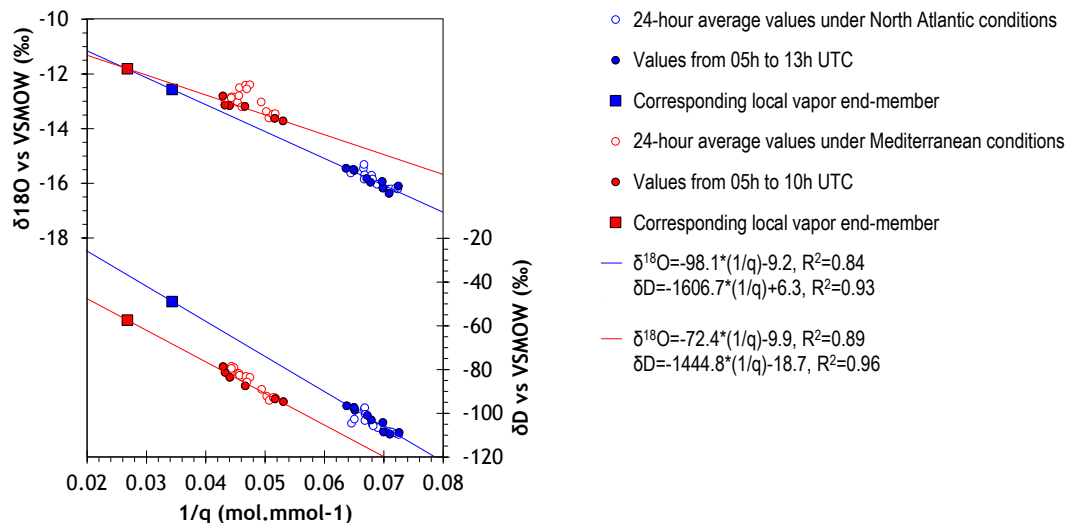
Figure 6. Relationships between 24 h average values of δ_v and $1/q$ according to the two main air mass origins, and corresponding linear regressions for the period of q increase (see text). Squares indicate the isotopic composition of the local vapor end-member calculated for a mixing ratio corresponding to saturation at the water surface temperature.

Legend in figure:
- ○ 24-hour average values under North Atlantic conditions
- ● Values from 05h to 13h UTC
- ■ Corresponding local vapor end-member
- ○ 24-hour average values under Mediterranean conditions
- ● Values from 05h to 10h UTC
- ■ Corresponding local vapor end-member
- — $\delta^{18}O = -98.1*(1/q) - 9.2$, $R^2 = 0.84$
  $\delta D = -1606.7*(1/q) + 6.3$, $R^2 = 0.93$
- — $\delta^{18}O = -72.4*(1/q) - 9.9$, $R^2 = 0.89$
  $\delta D = -1444.8*(1/q) - 18.7$, $R^2 = 0.96$

Axis labels: δ18O vs VSMOW (‰), δD vs VSMOW (‰), 1/q (mol.mmol-1)

Title Page

Abstract | Introduction

Conclusions | References

Tables | Figures

|◄ | ►|

◄ | ►

Back | Close

Full Screen / Esc

Printer-friendly Version

Interactive Discussion

Figure 7. 24 h average values of δ_v according to the two main air mass origins, corresponding linear regressions for the period of q increase (see text), and calculated local vapor end-member (see Fig. 6 for details). For reference, the LMWL is also plotted.

Legend:
- - - LMWL
- ○ 24-hour average values under North Atlantic conditions
- ● Values from 05h to 13h UTC
- ■ Corresponding local vapor end-member
- ○ 24-hour average values under Mediterranean conditions
- ● Values from 05h to 10h UTC
- ■ Corresponding local vapor end-member
- $\delta D = 15.2 * \delta^{18}O + 137.7$ ($R^2 = 0.94$)
- $\delta D = 18.5 * \delta^{18}O + 159.2$ ($R^2 = 0.93$)